CHAPTER-2

Characterization Techniques

2.1. Characterization techniques

The synthesized materials in our work were extensively characterized via the use of a wide range of experimental methods, yielding deep insights into their structural, chemical, thermal, and electrochemical characteristics. Fourier transform infrared spectroscopy (FTIR), which analyzed the infrared spectra to identify functional groups and chemical bonding within the material, were used to examine the optical and structural properties. X-ray diffraction (XRD), which provides details on the phase composition and crystallinity of the produced samples, was used to examine the crystallographic structure. Using high-resolution surface images from field-emission scanning electron microscopy (FE-SEM), the morphological characteristics and surface texture of the catalysts were examined. EDS and elemental mapping were used to perform elemental analysis, allowing for a quantitative knowledge of the composition and elemental distribution of the material.

The produced catalysts were characterized electrochemically using chronopotentiometry (CP), linear sweep voltammetry (LSV), cyclic voltammetry (CV), and electrochemical impedance spectroscopy (EIS) analyses. The OER performance was assessed using LSV, which recorded the current density as a function of applied potential. On the other hand, CV revealed information about the catalytic activity and redox behavior across a number of cycles. A thorough knowledge of the electrode-electrolyte interface and the effectiveness of electron transfer during OER was provided by the application of EIS to investigate the charge transfer resistance and general kinetics of the catalytic process. For the inspection of stability of the electrocatalyst, CP is conducted which is the variation of potential with time at constant current density.

The synthesized catalysts underwent *operando* spectro-electrochemical investigation in addition to structural and electrochemical characterizations to study the production and behavior of active intermediates during the OER. This cutting-edge method makes it possible to monitor the catalyst's reaction in real-time while it is operating, giving important information about the dynamic processes that take place on the catalyst surface during electrocatalysis. *Operando* approaches give the special benefit of probing the catalyst while the OER is actively occurring, so exposing the real intermediates that engage in the reaction mechanism. This is in contrast to ex situ methods, which record the condition of the material before or after the reaction.

In order to ensure a comprehensive characterization approach for advanced materials research, each of these techniques is covered in detail, offering a solid understanding of their principles, applications, and significance in assessing the overall properties and performance of the synthesized electrocatalysts.

2.2. Structural Analysis

2.2.1. Fourier transform infrared spectroscopy (FT-IR)

An effective method for obtaining the infrared spectra of solid, liquid, or gaseous materials in either the emission or absorption modes is fourier transform infrared spectroscopy (FT-IR). A material's spectrum may be measured between 4000 to 400 cm^{-1}, which allows for the identification of the different functional groups that are present in the sample. The fundamental idea behind FT-IR is the use of the fourier transform, a mathematical approach, to change the interferogram raw data into the real spectrum.

Functional groups in molecules function as dipoles in FT-IR, corresponding to certain vibrational energies. The material preferentially absorbs wavelengths with energies that coincide with the vibrational frequencies of the molecular bonds when it is subjected to infrared light in the 4000-400 cm^{-1} range. The remaining frequencies are then sent as a consequence. Every functional group has a different vibrational energy that is attributed to its specific atomic arrangement and binding strength. This energy is dependent on the bond's spring constant (k) and the reduced mass (μ) of the bound atoms. For every functional group and subcategory of functional groups, these characteristics produce distinct vibrational modes. Moreover, FT-IR is beneficial for evaluating nanomaterials, since functional groups bound to the surface of nanomaterials generally create different spectrum patterns compared to free functional groups. Because of this, FT-IR is a helpful technique for examining the surface chemistry of nanoparticles. Using the Thermo Scientific Nicolet 6700 FT-IR spectrometer **(Figure 2.1 (a))**, which operates in the 450–4000 cm^{-1} spectral region, we examined the surface chemistry and functional groups of the produced materials in this work.

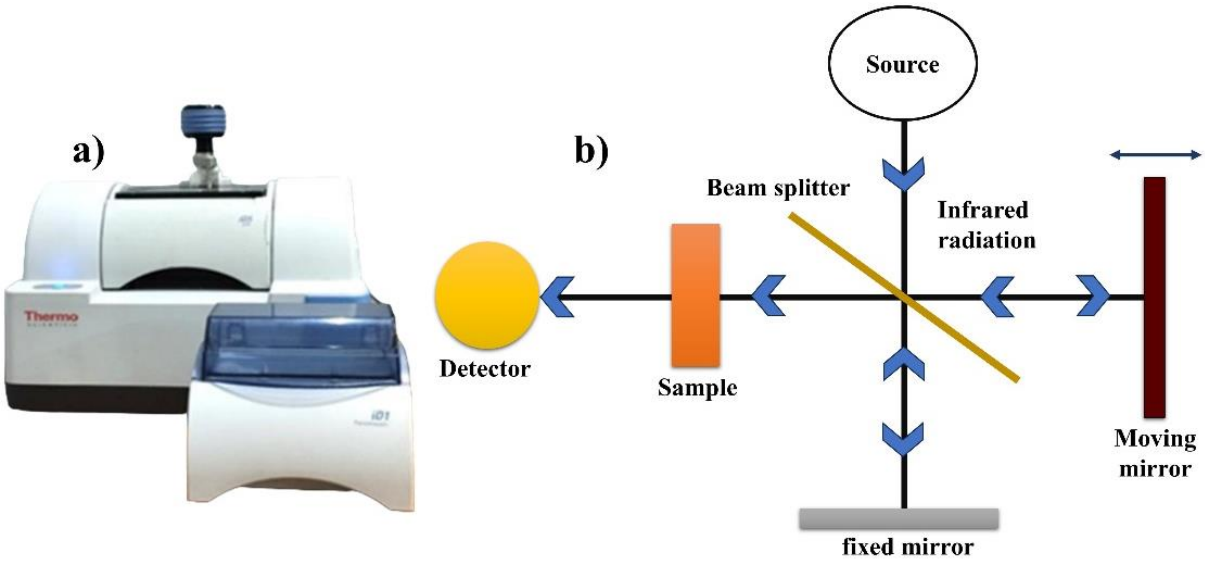

Figure 2.1 (a) Image of FT-IR spectrometer, **(b)** Michelson interferometer's operating principle.

FT-IR spectroscopy differs from conventional dispersive infrared spectroscopy in that it relies heavily on the Michelson interferometer **(Figure 2.1 (b))**. Monochromatic light is progressively focused onto the sample throughout a range of infrared wavelengths in dispersive infrared spectroscopy. On the other hand, non-dispersive FT-IR uses an interferometer to concurrently expose the sample to many IR frequencies; post-processing is then used to examine the transmitted light. When compared to traditional dispersive approaches, this methodology yields spectral data quicker and with higher accuracy.

2.2.2. X-Ray diffraction patterns (XRD)

A potent analytical method for learning in-depth details about the molecular arrangement and crystalline structure of both natural and artificial materials is X-ray diffraction (XRD). The method creates unique XRD patterns by using the constructive interference of monochromatic

X-rays with a crystalline substance. Strong monochromatic X-rays that are applied to a sample cause the crystal lattice to interact with the rays **(Figure 2.2 (b))** in accordance with Bragg's Law, that can be written as $n\lambda = 2d \sin\theta$. Where, d is the lattice spacing, diffraction angle is θ, and X-ray wavelength is λ. At certain angles, constructive interference produces diffracted beams.

The sample is scanned across a span of 2θ angles in order to get a full set of diffraction data, which enables the identification of different lattice planes. Upon being analyzed by detectors, the diffracted X-rays create a sequence of diffraction peaks that are unique to each material and correspond to certain d-spacings. A determination of the phase and crystallographic structure of the material may be made by comparing these diffraction patterns with reference standards. Using a Rigaku Miniflex 600 X-ray Diffractometer **(Figure 2.2 (a))** with Cu-Kα radiation (λ = 1.5405), the materials were examined for this investigation.

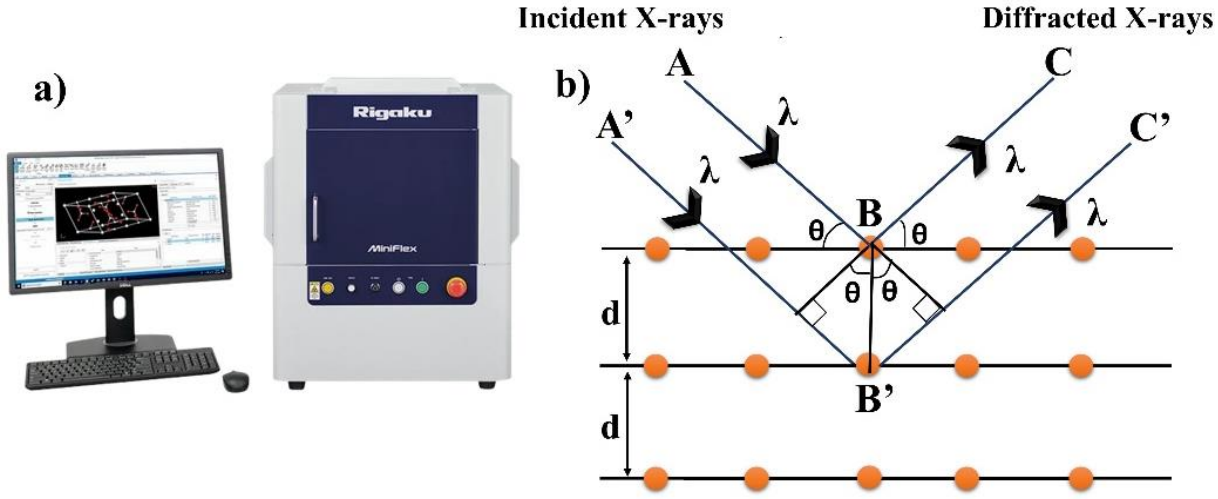

Figure 2.2 (a) Image of Rigaku Miniflex 600 diffractometer, **(b)** schematic illustration of X-ray beam diffraction through a crystalline material.

For the purpose of determining the quasi-lattice parameters, the diffractometer was calibrated using silicon powder, and single-crystal silicon was used as a reference to guarantee accurate 2θ observations. Using a step size of 3°/min, XRD data were collected throughout a 2θ range of 10 – 80°, with changes made as needed.

2.3. Morphological Analysis

2.3.1. Field-Emission Scanning Electron Microscopy (FE-SEM)

Compared to traditional scanning electron microscopy (SEM), field-emission scanning electron microscopy (FE-SEM) offers a wider energy range and a greater resolution, making it an effective method for obtaining comprehensive details on the structure and surface morphology of materials. A concentrated electron beam is employed in both FE-SEM and SEM to examine a sample's surface, however, the electron source is where the main distinction between the two is found. A field emission gun (FEG) on the FE-SEM produces a highly concentrated electron beam at both high and low energies. This property makes it possible for FE-SEM to attain noticeably better spatial resolution, which is essential for closely examining minute surface details.

The FE-SEM's capability to function at very low accelerating voltages, between 0.02 to 5.0 kV, is one of its primary benefits. This function helps to lessen the charging effects that may otherwise cause sample damage, which is especially helpful when evaluating non-conductive or sensitive specimens [1]. Because of this, FE-SEM is particularly helpful for researching materials that could be susceptible to high-energy electron beams, such as polymers and biological samples. The use of an in-lens detector, which enables the device to

take high-resolution pictures even at low accelerating voltages, is another unique characteristic of FE-SEM **(Figure 2.3 (b))**. The closer the in-lens detector is to the sample, the more efficiently signals are collected, improving the quality and clarity of the picture. Because of this, FE-SEM is a very useful technique for fields like semiconductor research, materials science, and nanotechnology that need precise surface imaging.

We used the FEI NOVA NANO SEM 450 model, a cutting-edge FE-SEM made in the USA, for our investigation. This device **(Figure 2.3 (a))** allowed us to closely inspect the surface characteristics of our samples, guaranteeing that even the smallest structural details were properly recorded and examined.

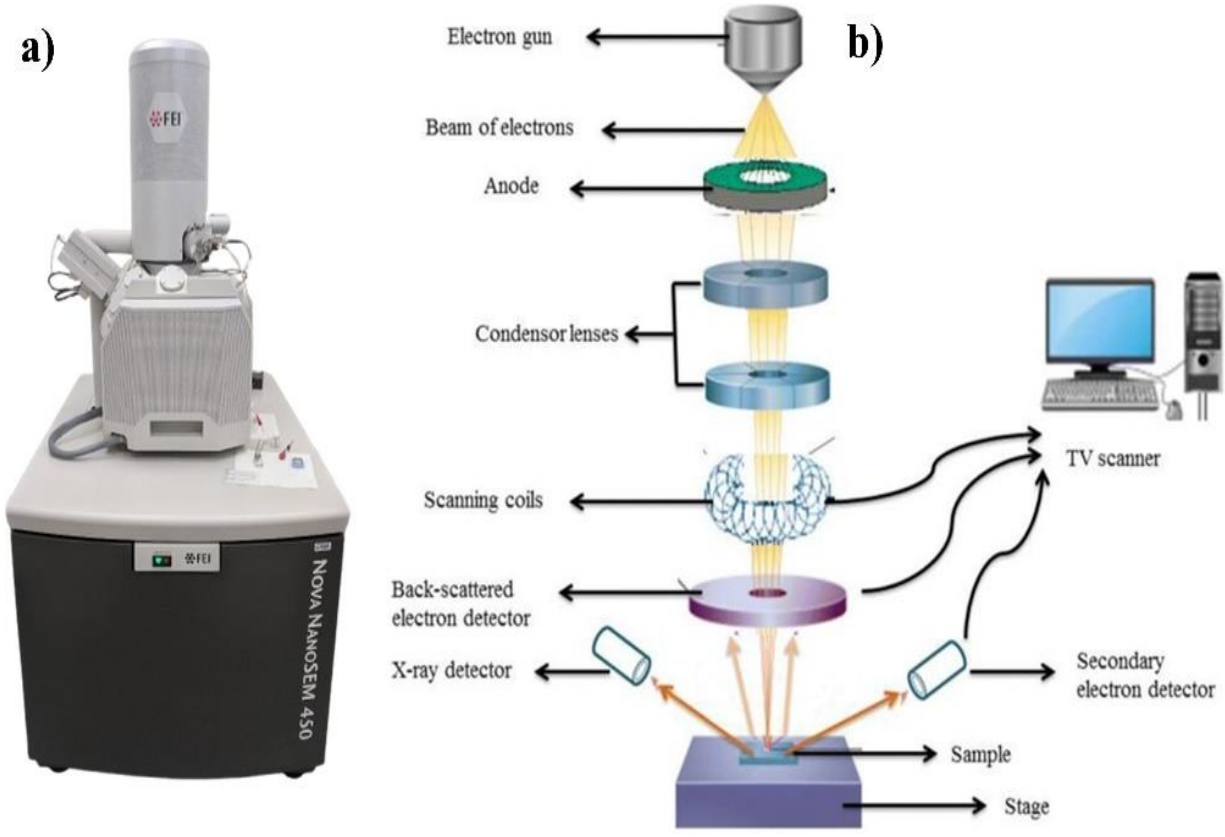

Figure 2.3 (a) Image of FE-SEM instrument, **(b)** components of the instrument [2].

2.3.2. High-Resolution Transmission Electron Microscopy (HR-TEM)

The highly advanced method known as transmission electron microscopy (TEM) makes it possible to see the internal structure of materials in great detail and at very high resolutions. In a transmission electron microscope (TEM), an ultra-thin specimen is passed through by a high-energy electron beam that interacts with the material it passes through. An image is created as a consequence of this interaction and is subsequently concentrated and enlarged onto an imaging device, which might be a digital sensor, a fluorescent screen, or a layer of photographic film.

The main benefit of TEM is that it uses electrons that have a shorter de Broglie wavelength than visible light, which makes imaging with much better resolution feasible than with traditional optical microscopes. Because of this, TEM may show very fine structural features that are much beyond the capability of even the most sophisticated optical microscopes, often on the atomic or sub-nanometer scale. The electrons are dispersed differently as they go through the specimen based on changes in the material's composition, thickness, or density. The resultant picture has contrast due to these variations in electron absorption, which offers a close-up look at interior structures. Understanding the complex interior architecture of specimens is essential in disciplines like materials science, biology, and nanotechnology, where TEM's capacity to detect minute differences in a sample's internal composition makes it an invaluable tool.

The interior structure of specimens is examined using TEM **(Figure 2.4 (a))**, that utilizes a high-energy electron beam which is accelerated by a high-voltage source. The electron beam passes via a vacuum chamber within the microscope and is produced by an

electron cannon that is mounted at the apex of the TEM column **(Figure 2.4 (b))**. This vacuum environment is essential because it keeps the electrons from interacting with the molecules of air, giving the electron beam an unobstructed route. The electron beam is focused into a narrow, very concentrated stream within the TEM by a number of condenser lenses. These lenses are crucial for regulating the diameter and thickness of the beam, which enables accurate electron concentration modification to maximize imaging efficiency. The electrons in this concentrated beam interact with an incredibly thin material as they go through or scatter off of it.

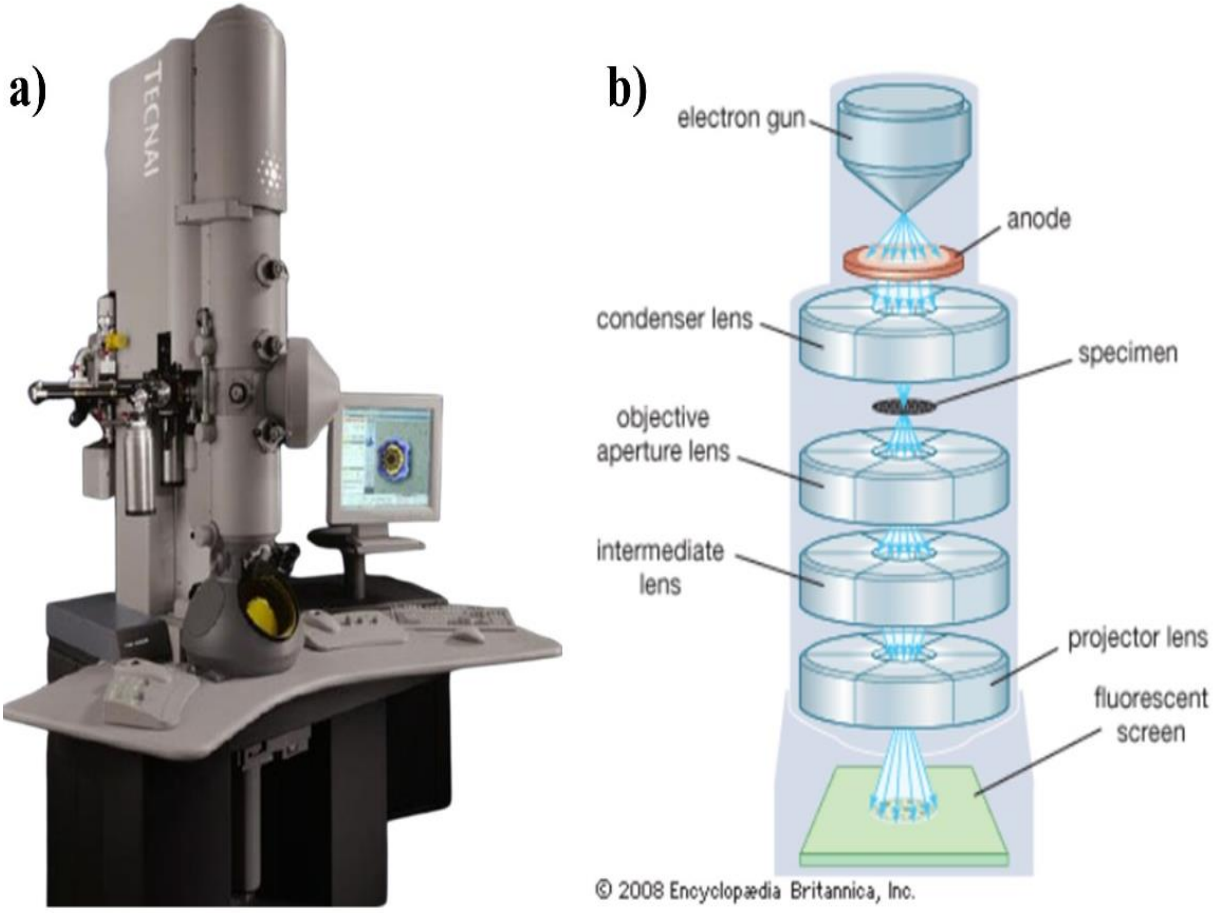

Figure 2.4 (a) HR-TEM instrument, **(b)** schematic diagram illustrating the components of a TEM microscope [3].

The electrons that continue ahead after exiting the material either hit a fluorescent screen or are picked up by a digital detector that is placed at the base of the microscope column [4]. differences in electron density are caused by the electrons' interactions with various specimen components, and these differences are converted into contrast on the imaging screen. Because less dense parts allow more electrons to flow through and look lighter, while denser portions appear darker owing to more electron absorption, this contrast exposes precise details of the sample's internal structure.

2.3.3. Selected Area Electron Diffraction Patterns (SAED)

With a transmission electron microscope (TEM), diffraction patterns from a specific area of a material are collected to create Selected Area Electron Diffraction (SAED) patterns. These patterns provide important insights on the phase, orientation, and crystallographic structure of materials at the nanoscale. In SAED, an aperture is employed to select a tiny, precise section of the sample, and the crystalline region inside this area is interacting with a focused electron beam. The periodic arrangement of atoms in the crystal scatters the electrons, projecting a diffraction pattern onto a digital detector or a fluorescent screen. The resultant pattern is made up of rings or spots that match the sample's crystallographic planes.

SAED patterns often take the form of distinct spots for single-crystal or well-aligned crystalline materials, where each spot denotes a distinct collection of crystallographic planes. The atomic plane spacing and the distance between these spots are connected, and the symmetry of the pattern may provide information about the crystal structure (e.g., cubic, hexagonal, tetragonal). We can ascertain the crystal structure of the sample and the lattice parameters by examining the location and intensity of the spots. Conversely, SAED patterns

that resemble concentric rings are produced by rocks that are polycrystalline or nanocrystalline. Every ring represents the average orientation of several randomly oriented tiny crystals and corresponds to a particular family of planes. The phase of the material may be determined by computing the d-spacing of these planes using the radii of the rings.

Amorphous materials' SAED patterns are quite different from crystalline materials' SAED patterns. Amorphous materials lack this long-range organization, while crystalline solids' periodic atomic arrangement results in well-defined patches or rings. Because of this, an amorphous material's SAED pattern usually takes the form of a wide, concentric ring or diffuse halo rather than sharp spots or clearly defined rings. This diffuse pattern represents the random dispersion of atoms in the amorphous phase, in which long-range atomic organization is not regular. A common cause of the wide halo is short-range order, in which atoms may be locally arranged into tiny clusters but lack a repeating pattern that spans more than a few atomic distances. The average interatomic distances inside the amorphous material may be inferred from the location and intensity of this diffuse ring.

In materials analysis, these SAED patterns are useful for differentiating amorphous phases from crystalline or polycrystalline phases. Materials with a lack of crystalline structure, glasses, and certain polymers are examples of materials that often exhibit amorphous SAED patterns.

2.4. Elemental Analysis

2.4.1. Energy dispersive X-ray Spectroscopy (EDS)

When figuring out a specimen's elemental composition, Energy Dispersive X-ray Spectroscopy (EDS) is a useful supplementary method that offers both qualitative and quantitative examination. When used in conjunction with scanning electron microscopy (SEM) and transmission electron microscopy (TEM) systems, EDS enables the identification of the elements contained in the sample as well as their relative abundances. Through the process, an EDS spectrum is produced, in which the X-ray energy released by the specimen upon interaction with the electron beam are represented by distinctive peaks for each element. Each element's concentration is indicated by the strength of these peaks.

EDS is especially helpful for surface examination and the investigation of thin layers or coatings since it can analyze the bulk concentration of elements at a short depth, usually between 50 and 100 nm. Because of such capabilities, EDS is a vital technique for material characterization, providing precise elemental information to supplement the structural data from TEM and SEM.

2.4.2. Elemental mapping

Elemental mapping is a potent analytical method for analyzing the spatial distribution of elements inside a material. It is carried out by combining energy dispersive X-ray spectroscopy (EDS) with scanning electron microscopy (SEM) or transmission electron microscopy (TEM). Using this method, we may learn more about the compositional arrangement of constituents

inside or on the surface of a specimen, leading to a more thorough comprehension of its chemical and microstructural characteristics.

The electron beam interacts with the material in SEM or TEM-based elemental mapping, resulting in the production of distinctive X-rays that are specific to each element that is present. These X-rays could be detected by the EDS detector, which then produces a spectrum that allows the elements to be identified by their distinctive energy peaks. EDS gathers data point-by-point by methodically scanning the electron beam over the specimen. This results in a comprehensive map that indicates the relative concentrations of various elements inside the sample as well as their locations. When examining materials with intricate compositions, such as alloys, ceramics, or biological tissues, elemental mapping is very helpful. This makes it possible to see phase borders, and to see how dopants or impurities are distributed, and chemical gradients. For understanding the characteristics of thin films, nanoparticles, and other nanoscale materials requires a knowledge of elemental distribution at the nanoscale.

Overall, EDS allows for elemental mapping, which visually displays the spatial distribution of individual elements across the sample, offering insights into the compositional variations.

2.5. Electrochemical Analysis

An overview of the essential elements and functions of an electrochemical workstation is given in this section. We used the USA made CHI-608C electrochemical analyzer/workstation **(Figure 2.5 (a))** for all electrochemical measurements in the investigation. Numerous electrochemical procedures, such as Open Circuit Potential (OCP), Electrochemical

Impedance Spectroscopy (EIS), Linear Sweep Voltammetry (LSV), Cyclic Voltammetry (CV) measurements, and Tafel analysis, can be carried out with this sophisticated instrument.

The CHI 608C is a potentiostat, which compute the current that passes between the working and counter electrodes and is intended to accurately adjust the potential difference between the working and reference electrodes. In this configuration, the measured response is the resultant cell current, and the applied cell potential is the controlled variable. This makes it possible to precisely characterize the system's electrochemical processes and characteristics.

A working electrode, a counter electrode, and a reference electrode comprise the three-electrode configuration used in an electrochemical cell for all experiments **(Figure 2.5 (b))**. The electrochemical processes of interest occur at the working electrode, current flows via the counter electrode to complete the circuit, and the reference electrode supplies a stable potential, which is used to determine the potential of the working electrode. This configuration is perfect for researching redox reactions, energy storage devices, and material characterization because it allows precise monitoring and control of electrochemical processes.

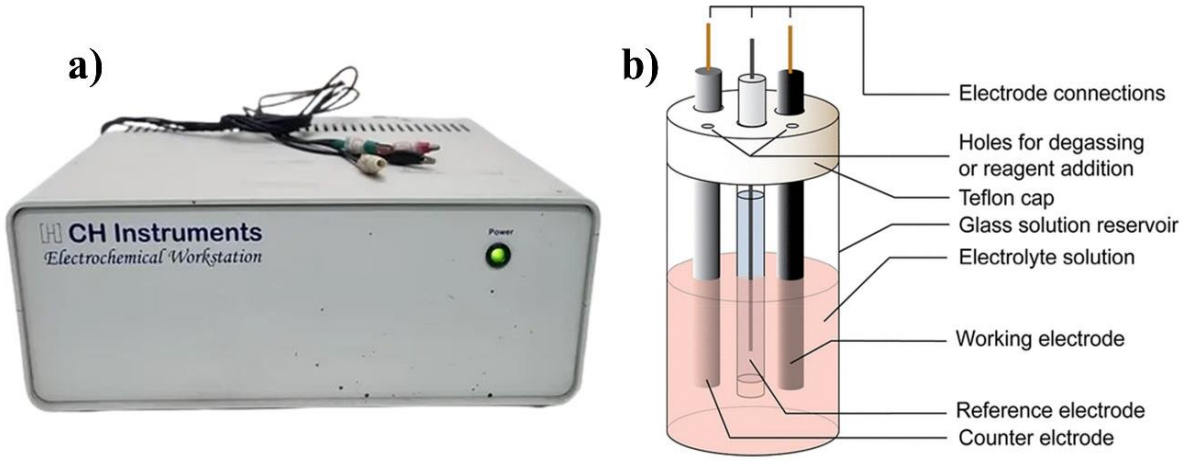

Figure 2.5 (a) CHI 608C electrochemical workstation, **(b)** electrochemical cell representation with a three-electrode setup [5].

2.5.1. Open-circuit potential (OCP)

The open-circuit potential (OCP) of an electrode refers to the potential at which there is a complete absence of net current flow between the electrode and its environment. A high-input-impedance voltmeter is usually used to measure this potential between the working electrode and a reference electrode, making sure that no external current is pulled from the working electrode during measurement. The cathodic (reduction) and anodic (oxidation) processes on the electrode surface are balanced at the OCP, which means that the rate of electron transport for each process is the same. Because of the exact offset between the opposing reactions, this equilibrium produces no net flow of current. In a system where a redox couple is present and other electroactive species do not substantially contribute to the current, the OCP is equal to the equilibrium potential for that particular redox couple as determined by the Nernst equation.

In these circumstances, the OCP is regarded as "well poised," which denotes that it maintains its stability throughout time and is resistant to little changes in the solution's conditions or composition. Because it represents the system's intrinsic electrochemical balance, its stability is essential for precise electrochemical investigation. Before adding any external potentials for further electrochemical operations, monitoring the OCP offers information about the redox behavior of the electrode material, its interactions with the electrolyte, and the stability of the system [6].

2.5.2. Cyclic Voltammetry (CV)

Cyclic voltammetry (CV) is a widely used electrochemical technique for investigating the redox properties of materials. It is especially useful for assessing how chemicals behave electrochemically, giving information on how they oxidize and reduce. In CV, a working electrode's potential is adjusted linearly over time at a regulated scan rate, and the current that results are then measured. The reason the method is called "cyclic" is because the potential is swept forward to a predefined value and then backward to the starting value, creating a cycle. As a consequence, a distinctive cyclic waveform of potential against time is produced, and a cyclic voltammogram is produced when the current is plotted against potential.

Figure 2.6 (a) depicts a typical cyclic voltammogram, with two distinct peaks: an oxidation peak in the upper half of the positive current zone and a reduction peak in the bottom half of the negative current region. The potential at which a material loses electrons is represented by the oxidation peak, while the potential at which a material gets electrons is represented by the reduction peak. Significant details on the redox processes, including the stability of the electroactive species, the reversibility of the reactions, and the kinetics of electron transfer, may be learned from the locations and forms of these peaks.

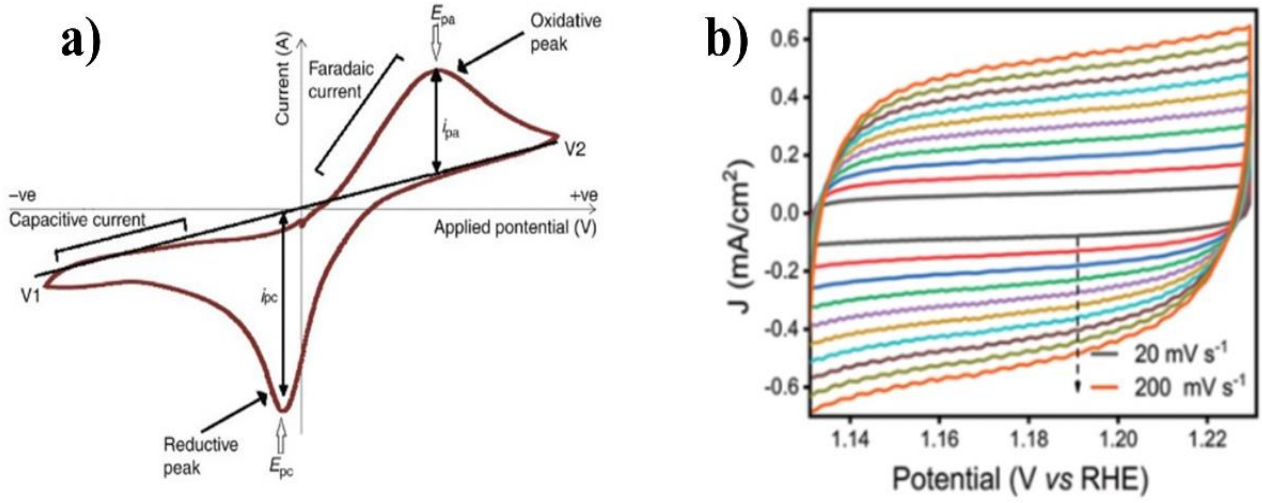

Figure 2.6 (a) Typical Cyclic Voltammogram [7], **(b)** CV in non-faradaic region [8].

Cyclic Voltammetry (CV) is frequently employed to evaluate the stability of the catalysts. The stability of OER electrocatalysts is a vital factor, reflecting the ability of a material to sustain its catalytic efficiency during repeated redox cycles. In this context, CV entails the systematic cycling of the working electrode's potential within a specified range that

encompasses the onset potential for the OER, all while meticulously documenting the resulting current.

Important signs of stability from CV data are the maintenance of peak current values, slight variations in the onset potential of the OER, and uniform electrochemical behavior across multiple scans. If a catalyst is prone to degradation, the CV curves may show a decrease in current with each cycle, a shift in the oxidation potential, or changes in peak shapes, which could indicate a loss of active sites or structural changes in the catalyst material.

CV conducted in the non-Faradaic region concentrates on potential ranges where no significant redox reactions occur. Instead of electron transfer reactions, the observed current in this region arises primarily from electrostatic processes, such as the charge and discharging of the electrical double layer at the electrode-electrolyte interface. In this region, when the potential of the working electrode is modified, the current is predominant due to the accumulation or depletion of charge at the electrode surface, without any electron transfer between the electrode and the species in the solution. The resultant current is often referred to as capacitive or double-layer charging current, as it is analogous to the charging of a capacitor.

The non-Faradaic region is essential in comprehending the double-layer capacitance of an electrode, which can yield insights into the surface area and porosity of the material, as well as the character of the electrode-electrolyte interface. For example, a higher capacitive current suggests a larger effective surface area, which is often desirable in applications like supercapacitors or for catalysts where a higher surface area can provide more active sites for reactions.

In a CV plot, the non-Faradaic region is typically characterized by a nearly rectangular or linear current response without distinct peaks **(Figure 2.6 (b))**, reflecting the absence of specific redox processes. This region is often observed before the advent of oxidation or reduction peaks, where the applied potential has not yet reached the range necessary to induce a redox reaction. By investigating the CV response in the non-Faradaic region, we can evaluate the intrinsic capacitive behavior of the material, providing baseline data for comparison when studying Faradaic.

2.5.3. Linear Sweep Voltammetry (LSV)

Linear Sweep Voltammetry (LSV) is an electrochemical method that may be viewed as a single directional sweep of a potential, representing half of a standard CV cycle. Unlike CV, which scans the potential back and forth, LSV includes applying a linearly variable potential between the working and reference electrode, moving from a defined lower potential limit to a higher potential limit at a fixed scan rate, and measuring the resultant current. As the potential rises, the current response is watched, and depending on the material's redox behavior and the selected potential range, either an oxidation peak or a reduction peak is recorded.

LSV is especially beneficial for understanding electrochemical processes such as the HER, OER, and ORR. For each of these reactions, LSV enables us to identify critical characteristics including onset potential (the potential where the reaction starts), current density, and the overall effectiveness of the electrocatalyst in driving the reaction. By concentrating on a single direction of potential change, LSV gives extensive information about the kinetics of electron transfer processes and the catalytic activity of materials under the

applied circumstances. This makes it a vital tool for improving catalysts for energy conversion applications, such as in fuel cells, electrolyzers, and batteries.

2.5.4. Electrochemical Impedance Spectroscopy (EIS)

Electrochemical Impedance Spectroscopy (EIS) is a flexible and well-established method for studying the complicated behaviors of electrochemical systems. It gives vital insights into the interfacial characteristics and dynamic processes that occur at the electrode-electrolyte contact. In EIS, an alternating current (AC) signal is delivered across an electrochemical cell, and the resultant impedance is evaluated across a large frequency range, generally from 10^5 Hz to 0.01 Hz. The results acquired from this test are commonly depicted visually using a Nyquist plot, as seen in **Figure 2.7**.

In a Nyquist plot, the real component of the impedance (Z_{real}) is displayed on the x-axis, while the imaginary component (Z_{imag}) is represented on the y-axis. This sort of graphic gives a visual depiction of numerous electrochemical processes happening at different frequency ranges. At higher frequencies, the Nyquist plot often displays a semicircular form, which is suggestive of charge transfer resistance (R_{ct}) paired with the uncompensated solution resistance (R_s). The R_{ct} refers to the resistance encountered during the electron transfer process at the electrode surface, representing the kinetics of electrochemical processes such as oxidation and reduction. The semicircle's diameter is directly connected to R_{ct}, with a bigger semicircle suggesting stronger resistance to charge transfer.

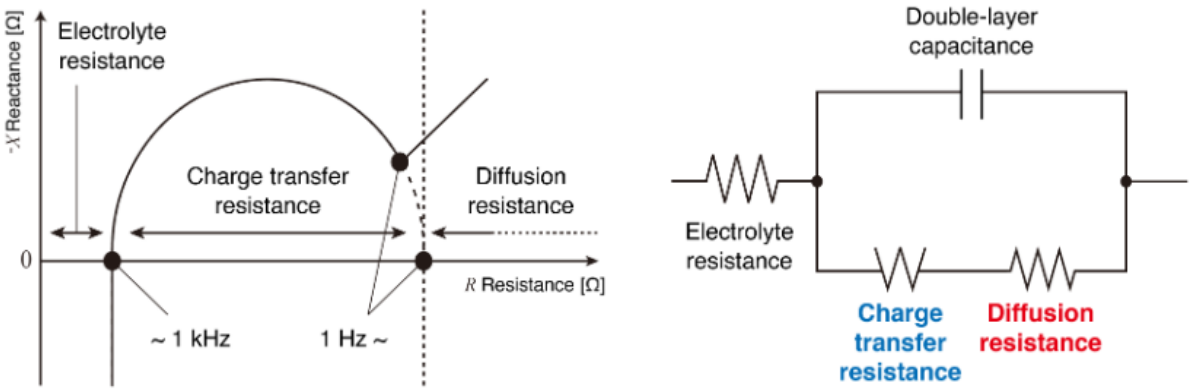

Figure 2.7 Nyquist plot and its equivalent circuit [9].

At lower frequencies, the Nyquist plot generally exhibits a linear zone, which corresponds to the diffusion-controlled processes in the system. This linear part, known as the Warburg impedance (W), indicates the resistance associated with the mass transit or diffusion of ions within the electrolyte. The slope of this linear component gives insights into the efficiency of mass transfer, where a steeper slope signifies a stronger barrier to ion diffusion. Together, the semicircle and the linear area offer a full perspective of both charge transfer kinetics and mass transport mechanisms inside the electrochemical system.

In addition to the Nyquist plot, EIS data may also be depicted using Bode charts, which give a supplementary viewpoint. A Bode plot illustrates the impedance magnitude and phase angle as functions of the logarithm of frequency. The impedance magnitude plot offers information on how the total impedance varies over the frequency range, while the phase angle plot illustrates the phase shift between the applied AC signal and the response. The Bode figure is especially helpful for differentiating distinct time constants in the system, since peaks in the phase angle indicate frequencies where capacitive or resistive processes dominate. For

example, a peak in the phase angle at a given frequency may coincide with the semicircular area in the Nyquist plot, revealing the frequency at which charge transfer resistance is most noticeable. Meanwhile, the slope of the magnitude plot at low frequencies might correspond with the Warburg area of the Nyquist plot, demonstrating the effect of diffusion processes.

Together, the Nyquist and Bode plots give a thorough insight of the electrochemical system's impedance characteristics, permitting extensive investigation of resistance, capacitance, and mass transfer processes at the electrode-electrolyte interface.

2.5.5. Chronopotentiometry (CP)

Chronopotentiometry is an electrochemical method in which a constant current is supplied to the working electrode during a given time period, while the resultant potential is continually measured as a function of time. Unlike approaches that alter the potential, chronopotentiometry focuses on examining how the electrode potential varies in response to a continuous current, offering insights into the behavior of the electrochemical system under regulated circumstances.

Chronopotentiometry is an excellent approach for testing the stability of electrochemical materials. For a stable material, the potential will stay largely constant or fluctuate gradually over time, showing that the material retains its structural integrity and active sites without considerable degradation. However, if the potential increases rapidly or displays abrupt variations, it may suggest deterioration of the electrode material, loss of active sites, or passivation of the surface. This instability might be due to corrosion, disintegration of the substance, or buildup of reaction intermediates that inhibit the process.

In the context of catalytic applications, chronopotentiometry may indicate the long-term durability of the catalyst under operating circumstances. For example, an increasing potential over time during OER may suggest that the catalyst is becoming less effective, needing greater overpotentials to maintain the same current owing to surface degradation or loss of catalytic activity.

2.6. *Operando* Spectro-electrochemical Analysis

Operando spectro-electrochemical analysis has evolved as a potent tool for analyzing the OER in real-time under operational conditions. This technology merges spectroscopic techniques with electrochemical measurements, enabling us to immediately see changes in the chemical composition, oxidation state, and structural dynamics of electrocatalyst materials as they are actively involved in the OER process. By providing a simultaneous view of both the electrochemical behavior and the corresponding spectroscopic signals, *operando* spectro-electrochemistry enables a deeper understanding of the mechanisms that govern the OER, including insights into intermediate species, catalytic pathways, and structural transformations.

In the context of OER, *operando* analysis may be conducted using several spectroscopic techniques such as Raman spectroscopy, X-ray absorption spectroscopy (XAS), infrared (IR) spectroscopy, or UV-Vis spectroscopy. For example, XAS may be used to monitor changes in the oxidation states of metal centers in transition metal oxides or hydroxides, which are frequent OER catalysts. Raman spectroscopy, on the other hand, may offer information regarding structural changes in catalyst materials, such as the formation of active oxyhydroxide species under applied potentials. The ability to see these changes in real-time is especially significant for OER investigations since the reaction includes the production and

transformation of intermediary species that might be short-lived and tough to identify using standard ex situ approaches. *Operando* spectro-electrochemical analysis allows for the identification of these intermediates and the investigation of their involvement in the catalytic cycle, offering insights into the genesis of catalytic activity and stability.

Additionally, operando analysis may be utilized to monitor catalyst degradation processes over time, demonstrating how the structure and composition of the active material vary during continuous operation. This is vital for building more durable and efficient catalysts for practical applications in water splitting and renewable energy technologies.

2.6.1. *Operando* UV-Vis Spectro-electrochemical Analysis

Operando spectro-electrochemical investigations had been done utilizing the Ocean Optics FLAME-T-XR1-ES assembly, which works across a wavelength range of 200 nm to 1025 nm. UV-Vis spectroscopy is a well-established method for examining the reaction kinetics of catalysts and their optical properties, especially those which are either homogenous or display molecular heterogeneity [10]. When UV-Vis spectroscopy is linked with electrochemical measurements, it is referred to as UV-Vis spectro-electrochemistry (SEC) [11–14]. In the context of UV-Vis SEC, the changes in oxidation states and concentrations of catalysts may be successfully observed by evaluating their characteristic absorption spectra. These spectrum shifts may be measured using the Lambert-Beer law, stated in the following **Equation 2.1**:

$$A = \in \times l \times c \qquad \textbf{(2.1)}$$

Where, A indicates the absorbance, ϵ is the molar extinction coefficient ($M^{-1}\,cm^{-1}$), l specifies the path length of the medium (in cm), and c is the molar concentration (in M).

In the UV-Vis SEC setup, absorbance is measured while concurrently measuring the current passing via the electrochemical circuit. This dual measurement allows for the connection of current responses with optical data, offering a thorough knowledge of the link between the applied potential, electrolyte conditions, and reaction kinetics. While UV-Vis SEC has generally been used to molecular systems, its value extends to electrode materials as well [15–17]. To explore particular redox processes, whether oxidation or reduction, UV-Vis SEC is commonly done inside a three-electrode cell arrangement [18]. This design provides fine control over the electrochemical environment while acquiring spectroscopic data.

In the instance of the OER, the formation of numerous intermediates is delicately represented in the spectro-electrochemical data. OER happens by a series of one-electron transfer processes, starting with the generation of hydroxyl radicals ($–OH^–$) and moving through a cascade of intermediates, including peroxo ($–OOH^–$) and superoxo ($–O^{2–}$, $–OO^{2–}$) species. By collecting these intermediate forms in real time, *operando* UV-Vis SEC gives substantial insights into the molecular routes of OER, enabling for a better understanding of catalyst performance and stability under operating settings. This detailed research is crucial for optimizing catalysts for energy conversion applications, such as in water splitting and other renewable energy technologies.

2.7. References

[1] A. Jaiswal, Graphitic Carbon Nitride and Carbon Composites for Electroand Photochemical Applications, (2022). https://idr-lib.iitbhu.ac.in/xmlui/handle/123456789/1969 (toegang verkry 16 Oktober 2024).

[2] N. Munir, M. Hanif, D.A. Dias, Z. Abideen, The role of halophytic nanoparticles towards the remediation of degraded and saline agricultural lands, Environ. Sci. Pollut. Res. 28 (2021) 60383–60405. https://doi.org/10.1007/s11356-021-16139-9.

[3] H.P. Stevenson, A.M. Makhov, M. Calero, A.L. Edwards, O.B. Zeldin, I.I. Mathews, G. Lin, C.O. Barnes, H. Santamaria, T.M. Ross, S.M. Soltis, C. Khosla, V. Nagarajan, J.F. Conway, A.E. Cohen, G. Calero, Use of transmission electron microscopy to identify nanocrystals of challenging protein targets, Proc. Natl. Acad. Sci. U. S. A. 111 (2014) 8470–8475. https://doi.org/10.1073/pnas.1400240111.

[4] P. Hawkes, C.B. Carter and D.B. Williams (eds.): Transmission electron microscopy, diffraction, imaging, and spectroscopy, J. Mater. Sci. 52 (2017) 2989–2994. https://doi.org/10.1007/s10853-016-0540-1.

[5] N. Elgrishi, K.J. Rountree, B.D. McCarthy, E.S. Rountree, T.T. Eisenhart, J.L. Dempsey, A Practical Beginner's Guide to Cyclic Voltammetry, J. Chem. Educ. 95 (2018) 197–206. https://doi.org/10.1021/acs.jchemed.7b00361.

[6] A. Bard, L. Faulkner, H. White, Electrochemical methods: fundamentals and applications, 2022. https://books.google.com/books?hl=en&lr=&id=Sct6EAAAQBAJ&oi=fnd&pg=PR21&ots=QV3mtaJ0NX&sig=DLfrR_jFcE_cWnGqn5_EbKOHFu0 (toegang verkry 06 Mei 2024).

[7] V. Climent, J.M. Feliu, Cyclic voltammetry, in: Encycl. Interfacial Chem. Surf. Sci. Electrochem., Elsevier, 2018: bll 48–74. https://doi.org/10.1016/B978-0-12-409547-2.10764-4.

[8] G. Solomon, A. Landström, R. Mazzaro, M. Jugovac, P. Moras, E. Cattaruzza, V. Morandi, I. Concina, A. Vomiero, NiMoO4@Co3O4 Core–Shell Nanorods: In Situ Catalyst Reconstruction toward High Efficiency Oxygen Evolution Reaction, Adv. Energy Mater. 11 (2021). https://doi.org/10.1002/aenm.202101324.

[9] T. Tools, Nyquist Plot for Impedance Measurement of Lithium-ion Batteries, Https://Www.Hioki.Com/in-En/Learning/Electricity/Nyquist.Html. (2021) 1–8. https://www.hioki.com/us-en/learning/electricity/nyquist.html (toegang verkry 17 Oktober 2024).

[10] L. Duan, F. Bozoglian, S. Mandal, B. Stewart, T. Privalov, A. Llobet, L. Sun, A molecular ruthenium catalyst with water-oxidation activity comparable to that of photosystem II, Nat. Chem. 4 (2012) 418–423. https://doi.org/10.1038/nchem.1301.

[11] J.J. Concepcion, M.K. Tsai, J.T. Muckerman, T.J. Meyer, Mechanism of water oxidation by single-site ruthenium complex catalysts, J. Am. Chem. Soc. 132 (2010) 1545–1557. https://doi.org/10.1021/ja904906v.

[12] S.B. Sinha, D.Y. Shopov, L.S. Sharninghausen, C.J. Stein, B.Q. Mercado, D. Balcells, T.B. Pedersen, M. Reiher, G.W. Brudvig, R.H. Crabtree, Redox Activity of Oxo-Bridged Iridium Dimers in an N,O-Donor Environment: Characterization of Remarkably Stable Ir(IV,V) Complexes, J. Am. Chem. Soc. 139 (2017) 9672–9683. https://doi.org/10.1021/jacs.7b04874.

[13] Z. Codolà, I. Gamba, F. Acuna-Parés, C. Casadevall, M. Clémancey, J.M. Latour, J.M. Luis, J. Lloret-Fillol, M. Costas, Design of Iron Coordination Complexes as Highly Active Homogenous Water Oxidation Catalysts by Deuteration of Oxidation-Sensitive Sites, J. Am. Chem. Soc. 141 (2019) 323–333. https://doi.org/10.1021/jacs.8b10211.

[14] L. Francàs, R. Matheu, E. Pastor, A. Reynal, S. Berardi, X. Sala, A. Llobet, J.R. Durrant, Kinetic Analysis of an Efficient Molecular Light-Driven Water Oxidation System, ACS Catal. 7 (2017) 5142–5150. https://doi.org/10.1021/acscatal.7b01357.

[15] C.A. Mesa, E. Pastor, L. Francàs, UV–Vis operando spectroelectrochemistry for (photo)electrocatalysis: Principles and guidelines, Curr. Opin. Electrochem. 35 (2022) 101098. https://doi.org/10.1016/j.coelec.2022.101098.

[16] Y.W. Choi, H. Mistry, B. Roldan Cuenya, New insights into working nanostructured electrocatalysts through operando spectroscopy and microscopy, Curr. Opin. Electrochem. 1 (2017) 95–103. https://doi.org/10.1016/j.coelec.2017.01.004.

[17] C.J. Jafta, A. Hilger, X.G. Sun, L. Geng, M. Li, S. Risse, I. Belharouak, I. Manke, A Multidimensional Operando Study Showing the Importance of the Electrode Macrostructure in Lithium Sulfur Batteries, ACS Appl. Energy Mater. 3 (2020) 6965–6976. https://doi.org/10.1021/acsaem.0c01027.

[18] K.J. Lee, N. Elgrishi, B. Kandemir, J.L. Dempsey, Electrochemical and spectroscopic methods for evaluating molecular electrocatalysts, Nat. Rev. Chem. 1 (2017). https://doi.org/10.1038/s41570-017-0039.